

International Journal of Modern Physics A  
© World Scientific Publishing Company

## A NUMERICAL EVALUATION OF VACUUM POLARIZATION TENSOR IN EXTERNAL CONSTANT MAGNETIC FIELDS

KEN-ICHI ISHIKAWA<sup>\*</sup>, DAIJI KIMURA<sup>b</sup>, KENTA SHIGAKI, ASAKO TSUJI

*Graduate School of Science, Hiroshima University,  
Higashi-Hiroshima, Hiroshima 739-8526, Japan*

*<sup>b</sup>General Education, Ube National College of Technology,  
Ube, Yamaguchi 755-8555, Japan*

Recently Hattori-Itakura have derived the full Landau-level summation form for the photon vacuum polarization tensor in external constant magnetic fields at one-loop level. The tensor has three different form factors depending on the tensor direction against the external magnetic field. The renormalization is not trivial because these form factors are expressed in terms of double or triple series summation forms. We give a numerical UV subtraction method which can be applied to numerically evaluate the form factors in external constant magnetic fields. We numerically investigate the photon vacuum polarization tensor in the form of the Landau-level summation and estimate the systematic errors coming from the truncation of the Landau-level summation. We find that the error is practically controllable at  $O(10^{-2})$  level for electrons and muons in strong magnetic fields expected in heavy ion collision experiments with experimentally feasible kinematic parameter regions.

*Keywords:* Strong magnetic field; Vacuum polarization.

PACS Nos.: 12.20.-m, 11.15.Bt

### 1. Introduction

Photon vacuum polarization is a fundamental tool to access the structure of quantum vacuum. Strong external electromagnetic fields could affect the structure of QED vacuum and cause various nonperturbative phenomena such as pair production via the Schwinger mechanism, electron-positron pair production from a photon, and vacuum birefringence of a photon *etc.*<sup>1-6</sup> There have been many theoretical works to evaluate the vacuum polarization tensor in strong electromagnetic fields to investigate these phenomena.<sup>7-12</sup> Especially heavy ion collision experiments at RHIC and LHC could generate very strong magnetic fields of order of  $eB \sim O(m_\pi^2)$ ,<sup>13,14</sup> which could affect the QCD phase structure via the various chiral magnetic effects.<sup>15,16</sup> These effects can be experimentally looked into only if the invariant masses and the transverse momenta are in the accessible regions by the detectors.<sup>17-24</sup> We aim at

<sup>\*</sup>ishikawa@theo.phys.sci.hiroshima-u.ac.jp

providing a quantitative assesment of the effects to allow evaluation of experimental feasibilities.

Recently Hattori-Itakura have obtained the full Landau-level summation form for the photon vacuum polarization tensor in external constant magnetic fields aiming for the vacuum birefringence of a photon<sup>25</sup> by strong magnetic fields. Their form is expressed in terms of double or triple series analytically. This is based on the summation on the Landau-level of virtual charged particles and the form is very suitable to investigate the threshold structure of single photon decaying into a charged particle-antiparticle pair trapped in the magnetic field. The photon propagation could be a detector for the existence of very strong magnetic fields expected in heavy ion collision experiments at RHIC and LHC.<sup>13,14</sup> The analytic form could be an important basis to discuss the polarization tensor in more realistic external fields.<sup>12</sup>

In Ref. 25 they have discussed the renormalization and the UV-structure of the form factors contained in the vacuum polarization tensor. However their subtraction is not suitable to evaluate the form factors numerically because the subtraction is defined between the series upper limit and the UV cut-off of the subtraction integral. We modify their subtraction preferable to the numerical evaluation of the vacuum polarization tensor.

This paper proceeds as follows. In the next section, we present the master formula for the vacuum polarization tensor in external constant magnetic fields written in the Schwinger's proper time integral. Our subtraction method and the Landau-level summation form are explained in Section 3. The convergence and the systematic errors from the truncation of the Landau-level sumamtion are discussed in Section 4. The numerical results with kinematic parameters accessible in the heavy ion collision experiments are given in Section 5. We summarize the paper in the last section.

## 2. Vacuum Polarization Tensor in External Constant Magnetic Fields

The vacuum polarization tensor  $\Pi^{\mu\nu}$  in external fields has the following tensor structure.

$$\Pi^{\mu\nu}(k) = \left( P^{\mu\nu} - P_{\parallel}^{\mu\nu} - P_{\perp}^{\mu\nu} \right) N_0(k) + P_{\parallel}^{\mu\nu} N_1(k) + P_{\perp}^{\mu\nu} N_2(k) \quad (1)$$

where  $k^{\mu}$  is the photon four-momentum and the projection tensors are defined by

$$P^{\mu\nu} = k^2 \eta^{\mu\nu} - k^{\mu} k^{\nu}, \quad P_{\parallel}^{\mu\nu} = k_{\parallel}^2 \eta_{\parallel}^{\mu\nu} - k_{\parallel}^{\mu} k_{\parallel}^{\nu}, \quad P_{\perp}^{\mu\nu} = k_{\perp}^2 \eta_{\perp}^{\mu\nu} - k_{\perp}^{\mu} k_{\perp}^{\nu}. \quad (2)$$

We define the external magnetic field  $\mathbf{B}$  is directed along  $z$ -axis and  $B_z = B > 0$ . The photon four momentum  $k^{\mu}$  and the metric  $\eta^{\mu\nu}$  are classified according to the direction of  $\mathbf{B}$  as follows.

$$k_{\parallel}^{\mu} = (k^0, 0, 0, k^3) = (\omega, 0, 0, k_z), \quad k_{\perp}^{\mu} = (0, k^1, k^2, 0) = (0, k_x, k_y, 0), \quad (3)$$

$$\eta_{\parallel}^{\mu\nu} = \text{diag}(1, 0, 0, -1), \quad \eta_{\perp}^{\mu\nu} = \text{diag}(0, -1, -1, 0), \quad (4)$$

$$k_{\parallel}^2 = (k^0)^2 - (k^3)^2 = \omega^2 - k_z^2, \quad (5)$$

$$k_{\perp}^2 = -(k^1)^2 - (k^2)^2 = -(k_x^2 + k_y^2) = -\mathbf{k}_{\perp}^2. \quad (6)$$

We consider Dirac fermions with unit charge  $e > 0$  and mass  $m$ . The one-loop contribution to the form factors,  $N_j$ 's ( $j = 0, 1, 2$ ), is given by

$$N_j = -\frac{\alpha}{4\pi} \int_{-1}^1 dv \int_{0-i\varepsilon}^{\infty-i\varepsilon} dz \left[ \tilde{N}_j(z, v) e^{-i\psi(z, v)\eta - i\phi(v; r, \mu)z} - \frac{1-v^2}{z} e^{-i\frac{z}{\mu}} \right], \quad (7)$$

$$\tilde{N}_0(z, v) = \frac{\cos(vz) - v \cot(z) \sin(vz)}{\sin(z)},$$

$$\tilde{N}_1(z, v) = (1-v^2) \cot(z), \quad (8)$$

$$\tilde{N}_2(z, v) = 2 \frac{\cos(vz) - \cos(z)}{\sin^3(z)},$$

$$\psi(z, v) = \frac{\cos(vz) - \cos(z)}{\sin(z)}, \quad (9)$$

$$\phi(v; r, \mu) = \frac{1 - (1-v^2)r}{\mu}, \quad (10)$$

where we introduce dimensionless parameters  $\mu$ ,  $r$ , and  $\eta$  defined by

$$\mu = \frac{eB}{m^2}, \quad r = \frac{k_{\parallel}^2}{4m^2}, \quad \eta = \frac{2q}{\mu}, \quad \text{with } q = \frac{\mathbf{k}_{\perp}^2}{4m^2}. \quad (11)$$

The  $z$  integration, originating from the Schwinger's proper time, should be carried out slightly lower line along with the real axis in the complex plane to have the Feynman propagator boundary condition.

All we want to know is the value of  $N_j$ 's with arbitrarily values for  $\mu$ ,  $r$ ,  $q$ . When  $0 < r < 1$  the both exponential factors in the integrand converge to zero on the lower quarter circle path with infinite radius. The integrand has no poles in the lower complex plane. Thus the  $z$  integral path can be continued to lower imaginary axis as  $z = -ix$  via the Cauchy's integral theorem. This yields the well converging double integration form for  $N_j$ 's. On the other hand, when  $1 < r$ , the  $z$  integral should be evaluated via the residue theorem.<sup>26, 27</sup> In this case the line integral is the closed path on the quarter sector in the first quadrant of the complex plane, and a difficulty arises when evaluating the residue of the integrand. The poles of  $\tilde{N}_j$ 's locate on  $z = n\pi$  ( $n = 1, 2, \dots$ ), where the phase factor  $\psi$  in Eq. (9) also has pole. This means that the residue at  $z = n\pi$  ( $n = 1, 2, \dots$ ) is indefinite except for the  $\eta = 0$  cases.

When  $\eta = 0$  (equivalently  $q = 0$ ) case the  $z$  integration can be analytically performed yielding the DiGamma functions. The form for  $N_1$  has been obtained in Ref. 28. Similar form can be obtained for both  $N_0$  and  $N_2$ .

4 *K.-I. Ishikawa, D. Kimura, K. Shigaki, A. Tsuji*

The Hattori-Itakura formula opens the way to evaluate  $N_j$ 's for  $\eta > 0$  with  $1 < r$ . They used other form factors defined by

$$\chi_0 = -N_0, \quad \chi_1 = -(N_1 - N_0), \quad \chi_2 = -(N_2 - N_0), \quad (12)$$

where the zero-field counter term is contained only in  $\chi_0$ . For  $\chi_1$  ( $\chi_2$ ) the subtraction occurs between  $\tilde{N}_1$  ( $\tilde{N}_2$ ) and  $\tilde{N}_0$ . They analytically expand the integrand of Eqs. (8)-(10) in terms of  $C_\ell^n(\eta)$  defined by

$$C_\ell^n(\eta) = e^{-\eta} \eta^n \frac{\ell!}{(\ell+n)!} (L_\ell^n(\eta))^2, \quad (13)$$

where  $L_\ell^n(\eta)$  is the associated Laguerre polynomial, and integrate both of the  $v$  and  $z$  integrals. The expansion yields the double series on  $n$  and  $\ell$ , where the indexes  $n$  and  $\ell$  correspond to the Landau-level of virtual fermions trapped in the external magnetic field in the one-loop diagram. The zero field counter term in  $\chi_0$  still remains in the integral form. The UV cancellation between the double series and the double integral is impossible numerically. Although  $\chi_1$  ( $\chi_2$ ) is completely expanded in the double series, the location of the UV-divergence in the series is not aligned well between  $\tilde{N}_1$  ( $\tilde{N}_2$ ) and  $\tilde{N}_0$ . Thus the UV cancellation is not trivial even if they are renormalized. Therefore we need a well organized renormalization method suitable for the numerical evaluation. In the next section we show our renormalization method.

### 3. Subtraction method and the Landau-level sum form

We rearrange Eq. (7) to the following form.

$$N_j = -\frac{\alpha}{4\pi} \int_{-1}^1 dv \int_{0-i\varepsilon}^{\infty-i\varepsilon} dz \left[ \tilde{N}_j(z, v) e^{-i\psi(z, v)\eta} \left( e^{-i\phi(v; r, \mu)z} - e^{-i\frac{z}{\mu}} \right) \right] \\ - \frac{\alpha}{4\pi} \int_{-1}^1 dv \int_{0-i\varepsilon}^{\infty-i\varepsilon} dz \left[ \left( \tilde{N}_j(z, v) e^{-i\psi(z, v)\eta} - \frac{1-v^2}{z} \right) e^{-i\frac{z}{\mu}} \right]. \quad (14)$$

The first line is UV finite and we can entirely expand it according to the Hattori-Itakura's expansion method. The second part of  $N_j$  corresponds to  $N_j$  at  $r = 0$ , for which  $z$  integral can be analytically continued to  $z = -ix$  yielding suitable forms for the numerical integration. We note that for  $N_2$  form factor the singularity of  $\tilde{N}_2$  is worse than others as it contains  $1/\sin^3(z)$ . This yields another difficulty for the numerical evaluation. To tame the difficulty we replace  $\tilde{N}_2$  with

$$\tilde{N}_2 = 2i \frac{1}{\sin^2(z)} \frac{\partial}{\partial \eta}, \quad (15)$$

for the first line of Eq. (14) before applying the Hattori-Itakura's expansion.

Applying the above prescription we obtain the following form for the form factors.

$$N_j = -\frac{\alpha}{4\pi} \sum_{n=0}^{\infty} C_n \sum_{\ell=0}^{\infty} \Omega_{j,\ell}^n(r, \eta, \mu) - \frac{\alpha}{4\pi} \int_{-1}^1 dv \int_0^{\infty} dx \left[ \left( \bar{N}_j(x, v) e^{\bar{\psi}(x, v)\eta} - \frac{1-v^2}{x} \right) e^{-\frac{x}{\mu}} \right], \quad (16)$$

where  $C_n = (2 - \delta_{n,0})$  and

$$\Omega_{0,\ell}^n(r, \eta, \mu) = [(1 - \delta_{n,0})C_\ell^{n-1}(\eta) + (1 + \delta_{n,0})C_{\ell-1}^{n+1}(\eta)] \mathcal{F}_\ell^n(r, \mu) - (n/\eta) [C_\ell^n(\eta) + C_{\ell-1}^n(\eta)] \mathcal{G}_\ell^n(r, \mu), \quad (17)$$

$$\Omega_{1,\ell}^n(r, \eta, \mu) = [C_\ell^n(\eta) + C_{\ell-1}^n(\eta)] (\mathcal{F}_\ell^n(r, \mu) - \mathcal{H}_\ell^n(r, \mu)), \quad (18)$$

$$\Omega_{2,\ell}^n(r, \eta, \mu) = 4 \frac{dC_\ell^n}{d\eta}(\eta) \mathcal{R}_\ell^n(r, \mu), \quad (19)$$

$$\bar{N}_j(x, v) = -i\tilde{N}_j(-ix, v), \quad \bar{\psi}(x, v) = -i\psi(-ix, v), \quad (20)$$

with  $C_{-1}^n(\eta) = 0$ . The functions,  $\mathcal{F}_\ell^n$ ,  $\mathcal{G}_\ell^n$ ,  $\mathcal{H}_\ell^n$ , and  $\mathcal{R}_\ell^n$ , are

$$\mathcal{F}_\ell^n(r, \mu) = \mu [F_\ell^n(r, \mu) - F_\ell^n(0, \mu)], \quad (21)$$

$$\mathcal{G}_\ell^n(r, \mu) = \mu [G_\ell^n(r, \mu) - G_\ell^n(0, \mu)], \quad (22)$$

$$\mathcal{H}_\ell^n(r, \mu) = \mu [H_\ell^n(r, \mu) - H_\ell^n(0, \mu)], \quad (23)$$

$$\mathcal{R}_\ell^n(r, \mu) = \int_{-1}^1 dv \left[ \Psi \left( \frac{S_{\ell+1}^n(v; r, \mu)}{2\mu} \right) - \Psi \left( \frac{S_{\ell+1}^n(v; 0, \mu)}{2\mu} \right) \right], \quad (24)$$

$$F_\ell^n(r, \mu) = \int_{-1}^1 dv \frac{1}{S_\ell^n(v; r, \mu)}, \quad (25)$$

$$G_\ell^n(r, \mu) = \int_{-1}^1 dv \frac{v}{S_\ell^n(v; r, \mu)}, \quad (26)$$

$$H_\ell^n(r, \mu) = \int_{-1}^1 dv \frac{v^2}{S_\ell^n(v; r, \mu)}, \quad (27)$$

$$S_\ell^n(v; r, \mu) = rv^2 - (n\mu)v + 1 - r + (2\ell + n)\mu - i\varepsilon, \quad (28)$$

where the  $z$  integration is performed and the Feynman's  $i\varepsilon$  prescription is restored to identify the absorptive part of these functions for the  $v$  integration. The function  $\Psi(z)$  is the DiGamma function. We follow the notation for  $F_\ell^n$ ,  $G_\ell^n$ , and  $H_\ell^n$  given by Ref. 25 and the  $v$  integration can be done analytically as given in Appendix A except for  $\mathcal{R}_\ell^n$ . The form of  $\mathcal{R}_\ell^n$  is inspired from Ref. 28 in which the analytic form for  $N_1$  with  $q = 0$  has been obtained.

The DiGamma function  $\Psi(z)$  has poles at  $z = 0$  and negative integers. When  $1 < r$  the argument  $S_{\ell+1}^n/(2\mu)$  of  $\Psi(z)$  in Eq. (24) could hit the singularities in integrating  $v$ . In order to extract the absorptive part of Eq. (24) we employ the recurrence formula,  $\Psi(z) = \Psi(z+1) - 1/z$ , until the argument becomes a non-zero

6 *K.-I. Ishikawa, D. Kimura, K. Shigaki, A. Tsuji*

positive number as

$$\Psi(z) = \Psi(z+1) - \frac{1}{z} = \dots = \Psi(z+K+1) - \sum_{k=0}^K \frac{1}{z+k}, \quad (29)$$

where  $K$  is a nonnegative integer chosen to satisfy  $z+K+1 > 0$ . Thus Eq. (24) becomes

$$\begin{aligned} \mathcal{R}_\ell^n(r, \mu) = & \int_{-1}^1 dv \left[ \Psi \left( \frac{S_{\ell+1+K+1}^n(v; r, \mu)}{2\mu} \right) - \Psi \left( \frac{S_{\ell+1+K+1}^n(v; 0, \mu)}{2\mu} \right) \right] \\ & - 2 \sum_{k \geq 0}^K \mathcal{F}_{\ell+1+k}^n(r, \mu), \end{aligned} \quad (30)$$

$$K = \begin{cases} -\text{Ceiling}[A_{\ell+1}^n] & (|n\mu/(2r)| < 1 \text{ and } A_{\ell+1}^n \leq 0) \\ -1 & (\text{otherwise}) \end{cases}, \quad (31)$$

$$A_\ell^n = \frac{1}{2\mu} \left[ 1 - r + (2\ell + n)\mu - \frac{(n\mu)^2}{4r} \right]. \quad (32)$$

The absorptive part is extracted as the sum of  $\mathcal{F}_\ell^n$  and the  $v$  integral can be numerically evaluated. When  $|(v^2 - 1)r/(2\mu)| < 0.01$  the integrand of Eq. (30) is evaluated using 8th order Taylor expansion to avoid loss of significant digits;

$$\Psi(z + dz) - \Psi(z) \simeq \Psi^{(1)}(z)dz + \Psi^{(2)}(z)\frac{(dz)^2}{2} + \dots + \Psi^{(8)}(z)\frac{(dz)^8}{8!}, \quad (33)$$

where  $\Psi^{(j)}(z)$  is the polygamma function of order  $j$ . To reduce the cost of numerical integrations at each  $\ell$  we can use the following recurrence formula for  $\mathcal{R}_\ell^n$ ;

$$\mathcal{R}_\ell^n(r, \mu) = \mathcal{R}_{\ell-1}^n(r, \mu) + 2\mathcal{F}_\ell^n(r, \mu). \quad (34)$$

The form factors below threshold ( $r < 1$ ) can be evaluated numerically for any  $0 < q$  by analytic continuation  $z = -ix$  in Eq. (7). The form factors in these region have been investigated in Ref. 29. The values from the double integral are compared to our numerical estimates from the Landau-level summation Eq. (16) to check the consistency.

With the vanishing transverse momentum ( $q = 0$ ), the  $z$  integral in Eq. (7) can be performed analytically. Karbstein *et al.*<sup>28</sup> have shown the analytic form for  $N_1$  with  $q = 0$ , which is the integral containing the DiGamma functions similar to Eq. (24). This form is valid for any  $r$ . We obtain similar analytic expressions for  $N_0$  and  $N_2$  with  $q = 0$  as given in Appendix B together with  $N_1$  with  $q = 0$ . We can check the validity of the numerical values from Eq. (16) with  $q = 0$  by comparing to the values from the DiGamma expressions, Eqs. (B.1)-(B.5) given in Appendix B, in the case of  $1 < r$ . Before going to the numerical evaluation, we discuss the convergence of the double sum of Eq. (16) by observing the asymptotic form in the next section.

#### 4. Asymptotic form of the double series

The asymptotic form for Eqs. (25)-(24) in  $1 \ll \ell$  is given by

$$\mathcal{F}_\ell^n(r, \mu) \sim \frac{r}{3\mu\ell^2} + O\left(\frac{1}{\ell^3}\right), \quad (35)$$

$$\mathcal{G}_\ell^n(r, \mu) \sim \frac{nr}{15\mu\ell^3} + O\left(\frac{1}{\ell^4}\right), \quad (36)$$

$$\mathcal{H}_\ell^n(r, \mu) \sim \frac{r}{15\mu\ell^2} + O\left(\frac{1}{\ell^3}\right), \quad (37)$$

$$\mathcal{R}_\ell^n(r, \mu) \sim -\frac{2r}{3\mu\ell} + \frac{5r(1 + (n+1)\mu) - 2r^2}{15\mu^2\ell^2} + O\left(\frac{1}{\ell^3}\right). \quad (38)$$

When  $\eta > 0$  the coefficient function  $C_\ell^n(\eta)$  and its derivative behave as

$$C_\ell^n(\eta) \sim \frac{1}{\pi\sqrt{\eta\ell}} e^{-\frac{n+1}{4\ell}} \cos^2(\Theta_\ell^n(\eta)),$$

$$\frac{dC_\ell^n}{d\eta}(\eta) \sim -\frac{1}{\pi\eta} e^{-\frac{n+1}{4\ell}} \sin(2\Theta_\ell^n(\eta)), \quad (39)$$

$$\Theta_\ell^n(\eta) = 2\sqrt{\eta\kappa_\ell^n} - \frac{\pi}{2} \left(n + \frac{1}{2}\right), \quad (40)$$

$$\kappa_\ell^n = \ell + \frac{n+1}{2}, \quad (41)$$

for  $\eta < 4\kappa_\ell^n$  with  $1 \ll \ell$ . This is followed by the asymptotic form for the Laguerre polynomials

$$L_\ell^n(\eta) \sim \frac{(\ell+n)!}{\ell!} \frac{e^{\eta/2}}{\sqrt{\pi}} (\kappa_\ell^n \eta)^{-n/2-1/4} \cos \Theta_\ell^n(\eta), \quad (42)$$

based on Bessel function expansion.<sup>30,31</sup>

$\Omega_{0,\ell}^n$  and  $\Omega_{1,\ell}^n$  are bounded by

$$\Omega_{j,\ell}^n \leq |\Omega_{j,\ell}^n| \sim O\left(\frac{1}{\ell^{5/2}}\right) \quad (\text{for } j = 0 \text{ and } 1). \quad (43)$$

This is slowly converging series at a fixed  $n$ . For  $\Omega_{2,\ell}^n$ , however, it does not seem to be absolutely convergent since  $|\Omega_{2,\ell}^n| \sim O(1/\ell)$ . The cancellation due to the oscillatory behavior of  $dC_\ell^n/d\eta$  or due to the sign mixture among terms with different  $n$  could occur for the convergence. The worst case is that the series for  $\Omega_{2,\ell}^n$  is asymptotic. We could not prove the convergence for  $\Omega_{2,\ell}^n$  with  $0 < \eta$  case.

From Eq. (13) the coefficient function  $C_\ell^n(\eta)$  and the derivative for  $\eta = 0$  become

$$C_\ell^n(0) = \delta_{n,0}, \quad (44)$$

$$\left. \frac{n}{\eta} C_\ell^n(\eta) \right|_{\eta=0} = (\ell+1)\delta_{n,1}, \quad (45)$$

$$\left. \frac{dC_\ell^n}{d\eta}(0) \right| = -(2\ell+1)\delta_{n,0} + (\ell+1)\delta_{n,1}. \quad (46)$$

Since these do not have damping factors for  $1 \ll \ell$  the series convergence becomes critical. We check the convergence of the double series explicitly in the following. For  $\Omega_{0,\ell}^n$  and  $\Omega_{1,\ell}^n$  with  $\eta = 0$ , the double sum converges as follows.

$$\begin{aligned} \sum_{n=0}^{\infty} C_n \sum_{\ell=0}^{\infty} \Omega_{0,\ell}^n &= 2 \sum_{\ell=0}^{\infty} (\mathcal{F}_\ell^1 - (2\ell + 1)\mathcal{G}_\ell^1) \\ &\sim \sum_{\ell \gg 1}^{\infty} \left[ \frac{2r}{5\mu\ell^2} + O\left(\frac{1}{\ell^3}\right) \right] < \infty, \end{aligned} \quad (47)$$

$$\begin{aligned} \sum_{n=0}^{\infty} C_n \sum_{\ell=0}^{\infty} \Omega_{1,\ell}^n &= (\mathcal{F}_0^0 - \mathcal{H}_0^0) + \sum_{\ell=1}^{\infty} 2(\mathcal{F}_\ell^0 - \mathcal{H}_\ell^0) \\ &\sim \sum_{\ell \gg 1}^{\infty} \left[ \frac{8r}{15\mu\ell^2} + O\left(\frac{1}{\ell^3}\right) \right] < \infty, \end{aligned} \quad (48)$$

For  $\Omega_{2,\ell}^n$  it becomes

$$\begin{aligned} \sum_{n=0}^{\infty} C_n \sum_{\ell=0}^{\infty} \Omega_{2,\ell}^n &= \sum_{\ell=0}^{\infty} [-4(2\ell + 1)\mathcal{R}_\ell^0 + 8(\ell + 1)\mathcal{R}_\ell^1] \\ &\sim \sum_{\ell \gg 1}^{\infty} O\left(\frac{1}{\ell^2}\right) < \infty, \end{aligned} \quad (49)$$

where the linear and logarithmic divergences are canceled among  $n = 0$  and  $n = 1$  terms. Thus the double series for  $\Omega_{2,\ell}^n$  is not absolutely convergent and the result depends on the ordering of the summation. When  $q = 0$  ( $\eta = 0$ ) and  $r < 1$  we observe a large discrepancy caused by the conditional convergence property between the Landau-level summation formula and the double integral formula numerically. Fortunately  $N_2$  with  $q = 0$  does not contribute to the polarization tensor as it is multiplied by the projection tensor  $P_{\perp}^{\mu\nu}$  which is identical to zero.

So far we do not discuss the convergence of the summation on  $n$  except for the case  $\eta = 0$ . To check the validity of the Landau-level summation form we compare the value to those evaluated with the other forms numerically instead of analytically. The comparison is possible in the following two regions.

- (A) Double integral form in  $r < 1$ .
- (B) DiGamma form with  $q = 0$ .

The double integral form is obtained by substituting  $z = -ix$  in Eq. (7). The DiGamma form is given in Appendix B. The integral is numerically evaluated using the double-exponential quadrature formula. We employ the program in Ref. 32 to evaluate the numerical integration not only for the above (A) and (B) but for Eqs. (30) and (16). The missing region for the validity check (A) and (B) is  $1 < r$  with  $q \neq 0$ .

Since the series coefficients  $C_\ell^n$  and  $dC_\ell^n/d\eta$  are independent from the choice of  $r$  and only a finite set of  $(n, \ell)$  induces the absorptive part in  $\mathcal{F}_\ell^n$ ,  $\mathcal{G}_\ell^n$ ,  $\mathcal{H}_\ell^n$  and  $\mathcal{R}_\ell^n$  for



Table 1. Parameter combinations we investigated. We use  $m_e = 0.5109989$  [MeV],  $m_\mu = 105.6583668$  [MeV],  $m_\pi = 139.57018$  [MeV],  $0 < k_{\parallel}^2 < 4^2$  [GeV<sup>2</sup>],  $0 < k_{\perp}^2 < 3^2$  [GeV<sup>2</sup>]. We take 401 (41) sample points for both  $r < 1$  and  $1 < r$  region at equal intervals.

Case	$[m, eB]$	$\ell_{\max}$	# of sample points for $r$	# of sample points for $q$
[a-1]	$[m_\mu, 10m_\pi^2]$	1000 2000, 4000, 8000	401 41	31 31
[b-1]	$[m_\mu, m_\pi^2]$	1000 2000, 4000, 8000	401 41	31 31
[c-1]	$[m_\mu, (1/10)m_\pi^2]$	1000 2000, 4000, 8000	401 41	31 31
[a-2]	$[m_e, 10m_\pi^2]$	1000 2000, 4000, 8000	401 41	31 31
[b-2]	$[m_e, m_\pi^2]$	1000 2000, 4000, 8000	401 41	31 31
[c-2]	$[m_e, (1/10)m_\pi^2]$	1000 2000, 4000, 8000	401 41	31 31

a finite  $r$ , the double series does not change the asymptotic form irrespective of the choice of  $r$ . Therefore we expect that if we have the validity in (A)  $r < 1$  region with a truncated double series, the same truncated series is also valid in  $1 < r$  region. The comparison of (B) provides a limited consistency check for the statement. In the next section we make the above comparison numerically.

## 5. Numerical Results

We employ Fortran 90 language to evaluate Eq. (16) in double precision. The double integral on  $x$  and  $v$  is evaluated by nesting the double-exponential quadrature formula subroutine.<sup>32</sup> In order to avoid the loss of significant digit in  $\overline{N}_j(x, v)$  ( $\overline{\psi}(x, v)$ ) near  $x = 0$  we use the 9th order (11th order) Taylor expansion form for  $x < 0.02$  respectively. To avoid the overflow of hyperbolic functions in  $\overline{N}_j(x, v)$  and  $\overline{\psi}(x, v)$  for  $1 \ll x$  we transform them to a well organized exponential form for  $10 < x$ .

The coefficient functions  $C_\ell^n$  and  $dC_\ell^n/d\eta$  are computed using the three-term recurrence formula based on the Laguerre polynomials during the summation on  $\ell$ . This means that we keep several last values of  $L_{\ell-1}^n$  and  $L_{\ell-2}^n$  etc. to compute  $C_\ell^n$  and  $dC_\ell^n/d\eta$  for  $\Omega_{j,\ell}^n$  to avoid the full re-computation of  $L_\ell^n$  at each  $\ell$ . The three-term recurrence formula and numerical method we employed is explained in Appendix D.

The double series of Eq. (16) must be truncated at a cutoff index ( $n_{\max}, \ell_{\max}$ ) for the numerical evaluation. The summation on  $\ell$  is truncated at a  $\ell_{\max}$  independent of  $n$ . While the summation on  $n$  is stopped when the partial sum  $\delta N_j = \sum_{\ell=0}^{\ell_{\max}} \Omega_{j,\ell}^n$  becomes negligible compared to the current estimate of  $N_j$  provided by the following condition;

$$(|\delta N_j| < 10^{-14} \quad \text{and} \quad |N_j| < 10^{-14}) \quad \text{or} \quad |\Delta N_j|/|N_j| < 10^{-14} \quad (50)$$

in double precision arithmetic.

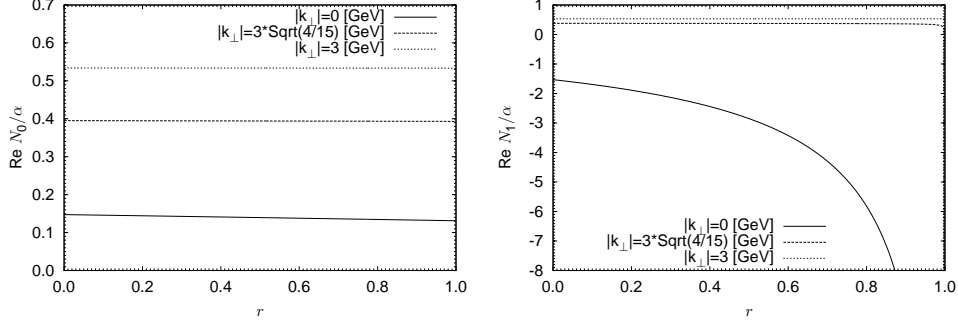


Fig. 1. Form factors  $N_0$  (left) and  $N_1$  (right) for muons (case [a-1]) in  $r < 1$  with  $\ell_{\max} = 1000$ .

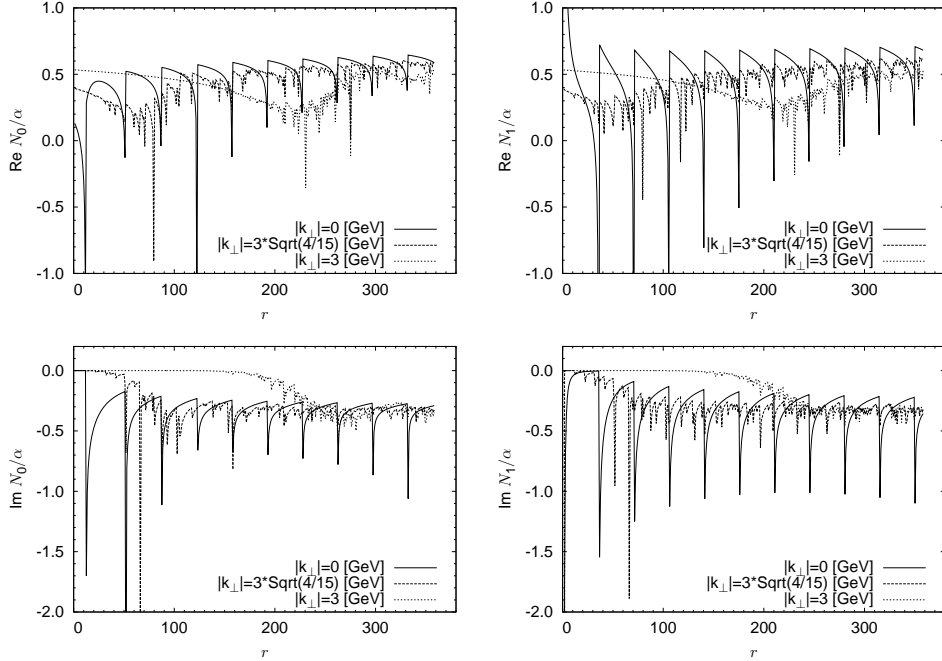


Fig. 2. Same as Fig.1 but for real (top) and imaginary (bottom) parts in  $1 < r$ .

We show the combination of input parameters for the form factors in Table 1. We choose the magnetic field strength at  $O(m_\pi^2)$  which is expected to exist in the heavy ion collisions at LHC.<sup>13,14</sup> The longitudinal and transverse momenta ranges we investigated are  $0 < k_{\parallel}^2 < 4^2$  [GeV<sup>2</sup>] and  $0 < \mathbf{k}_{\perp}^2 < 3^2$  [GeV<sup>2</sup>] respectively.

Figs. 1-3 show the form factors  $N_0$ ,  $N_1$  and  $N_2$  with  $m = m_\mu$  and  $eB = 10m_\pi^2$  (case [a-1]). The upper limit on  $\ell$  is  $\ell_{\max} = 1000$ . Figs. 4-6 are for electrons  $m = m_e$  with  $eB = 10m_\pi^2$  and  $\ell_{\max} = 1000$  (case [a-2]). Complicated threshold structures due to the Landau-levels are seen for  $1 < r$  in Figs. 2-3 and in Figs. 5-6. The solid

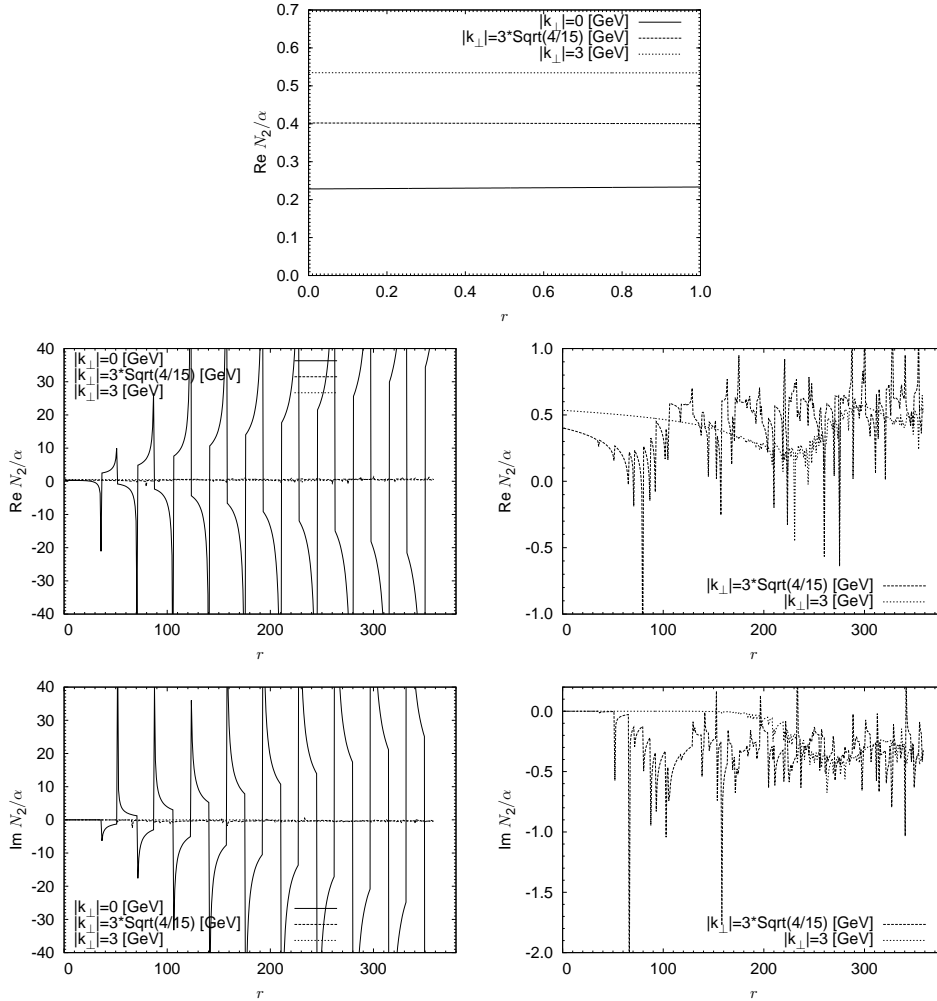


Fig. 3. Form factor  $N_2$  for muons (case [a-1]) with  $\ell_{\max} = 1000$  (top ( $r < 1$ ), middle (real part in  $1 < r$ ) and bottom (imaginary part in  $1 < r$ )). Right panels in  $1 < r$  are magnification of left panels.

lines in the top panels of Figs. 3 and 6, which correspond to  $N_2$  with  $q = 0$ , have a different behavior compared to the other lines. This is because of the conditionally convergent property of  $\Omega_{2,\ell}^n$  as explained in the last section. Thus the solid lines in the real part of  $N_2$  in  $1 < r$  (middle and bottom left panels of Figs.-3 and 6) also contain the same systematic error.

The truncation on the summation  $n$  is monitored as shown in Fig. 7. It requires 360–370 terms on  $n$  for larger transverse momenta  $q$ . We also observe  $n_{\max}$  depends linearly on  $\sqrt{\ell_{\max}}$  resulting  $n_{\max} = 920\text{--}940$  at  $\ell_{\max} = 8000$ . We observe a similar behavior on  $n_{\max}$  for electrons except for  $N_1$ . An early truncation in  $r \lesssim 1$  for

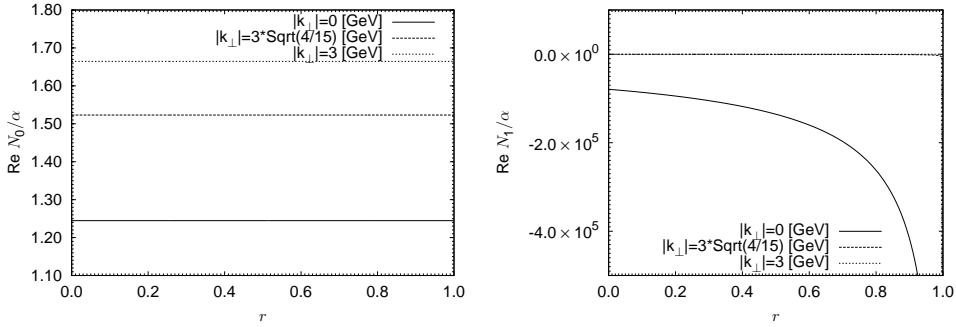


Fig. 4. Form factors  $N_0$  (left) and  $N_1$  (right) in  $r < 1$  for electrons (case [a-2]) with  $\ell_{\max} = 1000$ .

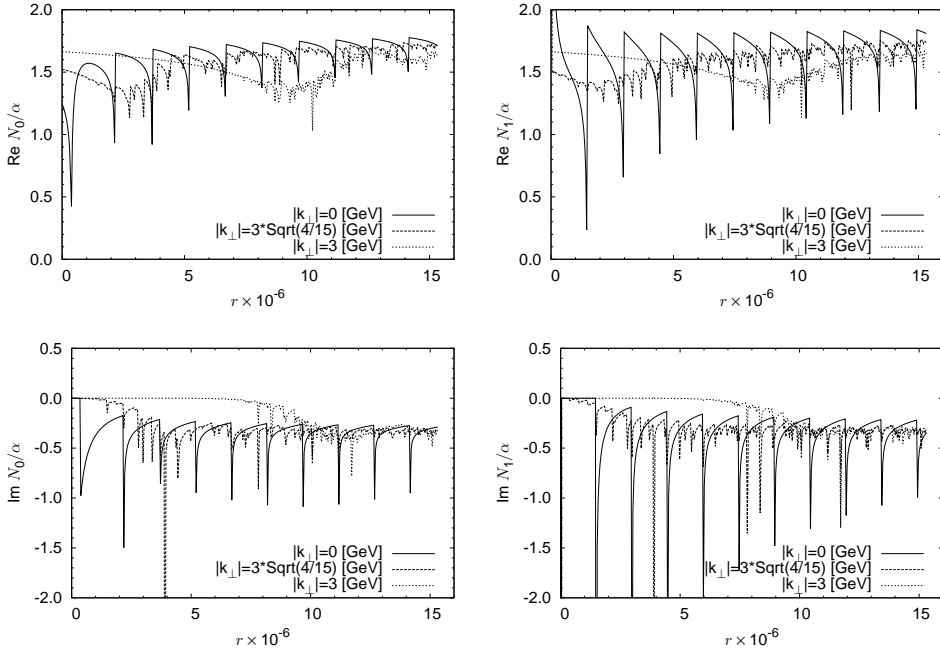


Fig. 5. Same as Fig.4 but for real (top) and imaginary (bottom) parts in  $1 < r$ .

$N_1$  is seen as it is well approximated by the lowest Landau level approximation.<sup>33</sup> As we decreasing  $eB$  to  $m_\pi^2/10$ ,  $n_{\max}$  increases to 5460–5500 (with  $\ell_{\max} = 1000$ ) for both electrons and muons. To approach the zero field limit we must accumulate more contributions from higher Landau levels. Verifying the zero field limit becomes difficult numerically. The zero field limit for the imaginary parts with  $q = 0$  can be analytically taken as shown in Appendix C.

The left panels in Fig. 8 show the discrepancy between the Landau-level form and the double-integral form as the consistency check (A) in  $r < 1$  for muons with  $eB =$

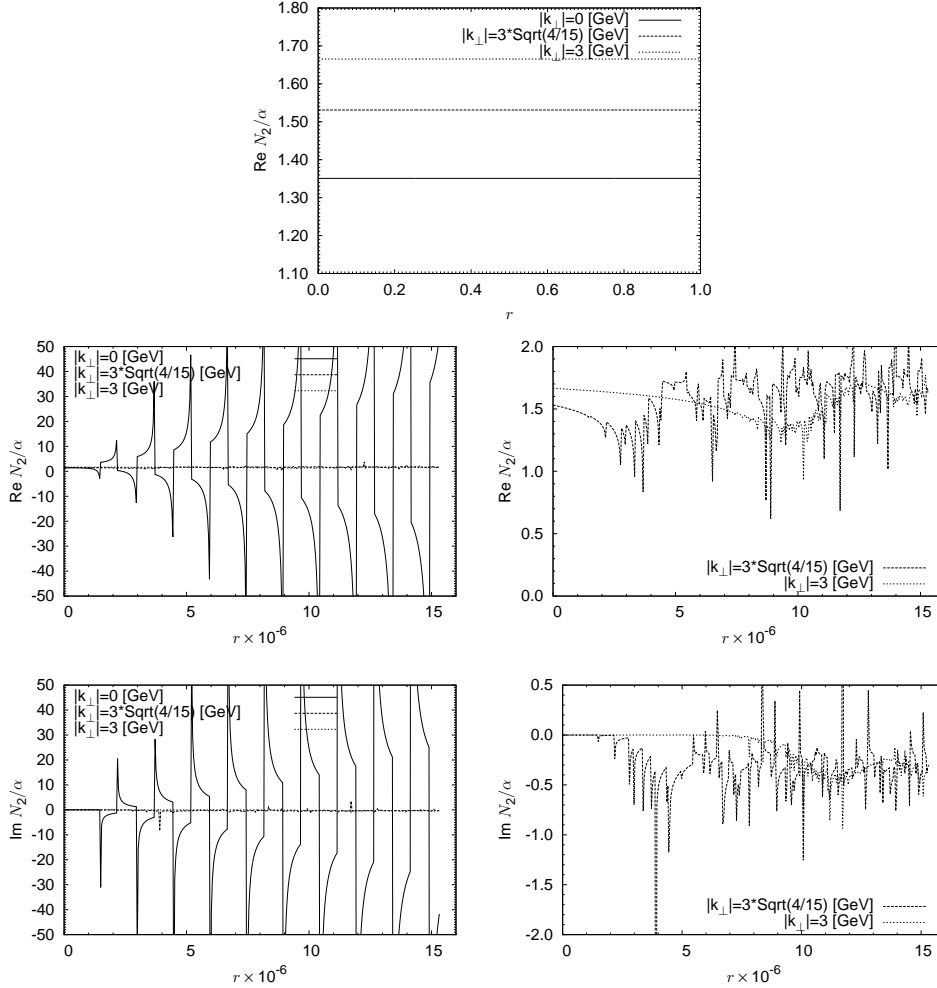
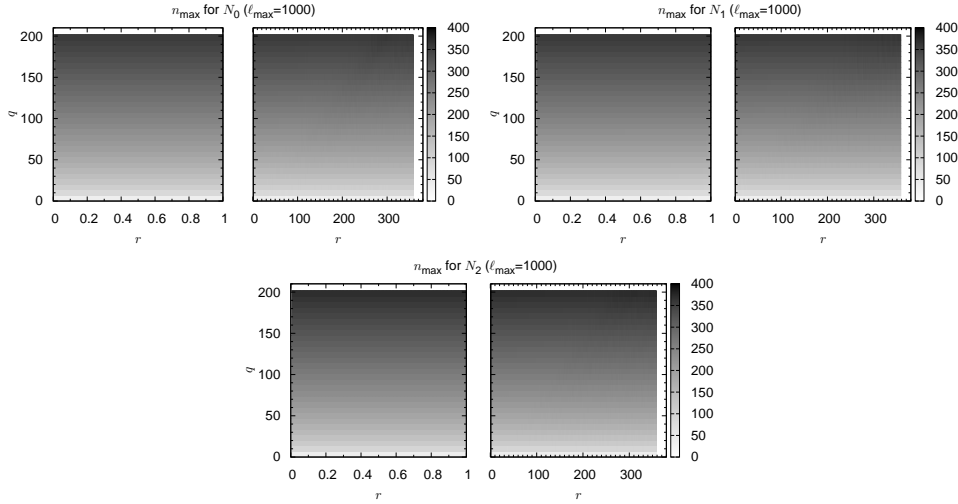


Fig. 6. Same as Fig.4 but for  $N_2$ .

$10m_\pi^2$  and  $\ell_{\max} = 1000$  (case [a-1]). The discrepancies  $\Delta N_0$  and  $\Delta N_1$  is at  $O(10^{-6})$  and decreases as increasing  $q$ . This is practically satisfactory level. While for  $\Delta N_2$ , the discrepancy with  $q = 0$  (solid line) has a  $O(1)$  error and it rapidly decreases to  $O(10^{-4})$  as increasing  $q$ . The truncation errors depend on  $r$  linearly, which is consistent with our asymptotic analysis. For electrons with  $eB = 10m_\pi^2$  (case [a-2]) we observe the same behavior in  $r < 1$  except for  $N_1$ . Since the relative truncation error  $|(\Delta N_1)/N_1|$  for electrons reaches the limit of double precision accuracy, we cannot extract the proper  $r$  dependence for  $\Delta N_1$  (case [a-2]).

The right panels in Fig. 8 show the discrepancy between the Landau-level form and the DiGamma form in  $1 < r$  with  $q = 0$  as the consistency check (B) for


 Fig. 7.  $n_{\max}$  for muons (case [a-1]) with  $\ell_{\max} = 1000$ .

muons with  $eB = 10m_\pi^2$  and  $\ell_{\max} = 1000$  (case [a-1]). The imaginary parts perfectly coincide with for all form factors. The real parts for  $N_0$  and  $N_1$  are linearly continued from the left panels and still remain below  $O(10^{-4})$  in the region we investigated. For  $\Delta N_2$ , however, it reaches  $O(1)$ . If we extend the observation in the region  $r < 1$  to the region  $r > 1$ , we expect even with  $q > 0$  that  $\Delta N_0$  and  $\Delta N_1$  still remain at  $O(10^{-4})$  and  $\Delta N_2$  with  $|\mathbf{k}_\perp| \gtrsim 3\sqrt{4/15} \sim 1.5$  [GeV] remains at  $O(10^{-2})$  (see Fig. 9).

The  $q$  dependence of the truncation error at  $r = 0.8$  with  $\ell_{\max} = 1000$  is shown in the left panels of Fig. 10 for the case [a-1].  $\Delta N_0$  and  $\Delta N_1$  behave as a linear function of  $\sqrt{q}$  while  $\Delta N_2$  behaves as a linear function of  $1/\sqrt{q}$  as shown by the fit lines in the figures. The  $\ell_{\max}$  dependence of the truncation errors at  $r = 0.8$ ,  $|\mathbf{k}_\perp| = 3\sqrt{14/15}$  [GeV] is shown in the right panels of Fig. 10 for the case [a-1]. The truncation error for  $N_0$  and  $N_1$  can be fitted with  $(c + d/\sqrt{\ell_{\max}})/\ell_{\max}$ .  $\Delta N_2$  can be fitted with  $c/\sqrt{\ell_{\max}} + d/\ell_{\max}$ . The same behavior is observed for other  $q$  in  $r < 1$ . This behavior cannot not be understood from the asymptotic behavior on  $\ell$  at a fixed  $n$  because it involves the truncation effect on the  $n$  summation.

With the global analysis for all cases shown in Table 1, we find that the truncation error can be well expressed by

$$\Delta N_j/\alpha = \left( c_j + d_j \sqrt{\frac{q}{\ell_{\max}}} \right) \frac{r}{\ell_{\max}} \quad (j = 0 \text{ and } 1), \quad (51)$$

$$\Delta N_2/\alpha = \left( c_2 + d_2 \sqrt{\frac{\ell_{\max}}{q}} \right) \frac{r}{\ell_{\max}}, \quad (52)$$

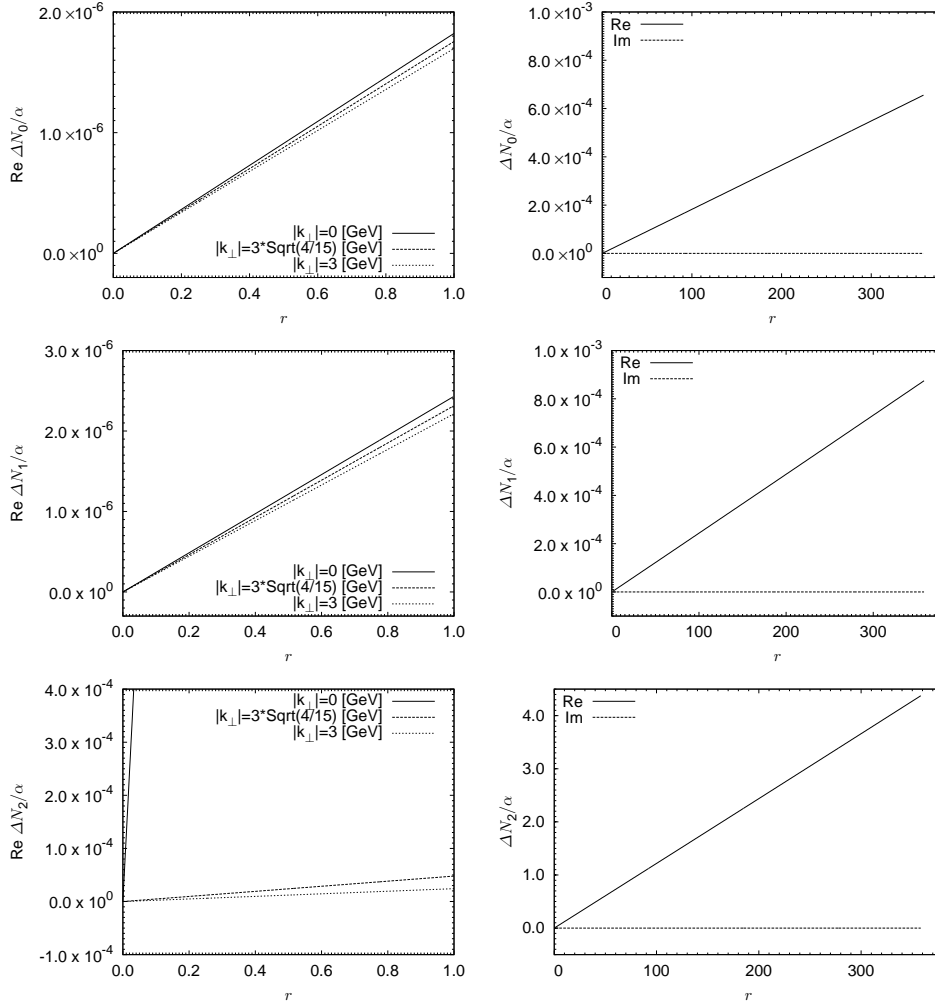


Fig. 8. Comparison (A) (left panels) and (B) (right panels) for muons (case [a-1]) with  $\ell_{\max} = 1000$

in  $r < 1$  derived from check (A), and by

$$\Delta N_j/\alpha = e_j \frac{r}{\ell_{\max}} \quad (j = 0 \text{ and } 1), \quad (53)$$

in  $1 < r$  derived from check (B).

Table 2 shows the coefficients for Eqs. (51)-(53) obtained by fitting all data from the parameter sets shown in Table 1. For electrons in strong magnetic fields  $eB = 10m_\pi^2$  and  $m_\pi^2$  we cannot determine  $c_1$  and  $d_1$  properly by fitting as  $|\Delta N_1/N_1|$  in  $r < 1$  reaches at double precision limit  $10^{-14}$ - $10^{-15}$ . We note that  $\Delta N_0$  and  $\Delta N_1$  with  $q = 0$  give upper bound for the truncation errors since the coefficients  $d_0$  and  $d_1$  are negative. As seen from Table 2  $c_0$  and  $e_0$  ( $c_1$  and  $e_1$ ) are consistent except

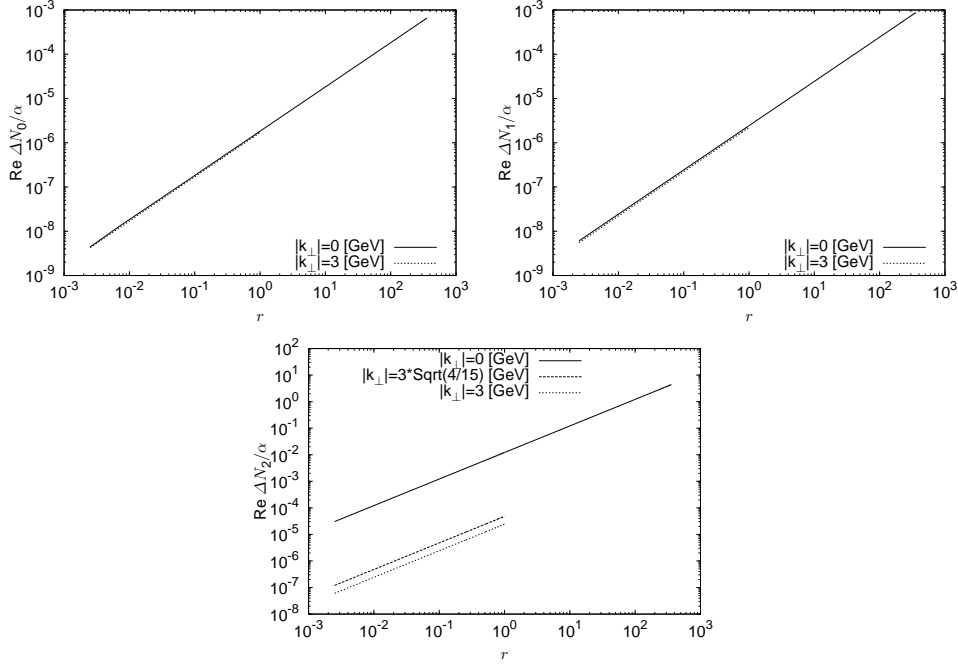


Fig. 9. Figs. 8 are combined in log-log plots (case [a-1] with  $\ell_{\max} = 1000$ ).

for the cases at  $eB = m_\pi^2/10$  (cases [c-1] and [c-2]). This is because the truncation error deviates from the function form Eq. (53). Thus the truncation errors for  $N_0$  and  $N_1$  can be directly estimated from the comparison (B) in  $1 < r$  region for sufficiently strong fields. We extend Eq. (52) determined by fitting in  $r < 1$  to estimate the truncation error  $\Delta N_2$  in  $1 < r$ . This gives an upper bound for  $\Delta N_2$  because it monotonically decreases as increasing  $q$ .

A practical algorithm to compute the form factors is summarized as follows;

- (1) Use double integral forms for all  $N_j$  in  $r < 1$ .
- (2) Use Landau level summation forms in  $1 < r$  for  $N_0$  and  $N_1$  with the truncation control by Eq. (53).
- (3) Use Landau level summation forms in  $1 < r$  for  $N_2$  with the truncation control by Eq. (52).

For muons in strong magnetic fields  $eB = m_\pi^2 - 10m_\pi^2$ , summation up to  $\ell_{\max} \simeq 10000-20000$  yields  $\sim 10^{-4}$  accuracy for  $N_0$  and  $N_1$ , and  $\sim 10^{-2}$  accuracy for  $N_2$  in the kinematic region;  $1 \text{ [GeV]} < |\mathbf{k}_\perp|$  and  $0 < k_\parallel^2 < 4^2 \text{ [GeV}^2]$ .

For form factors, especially for  $N_2$ , in weaker magnetic fields or with more precise values, it becomes difficult to obtain accurate form factors with our naive summation method. We might need to apply series acceleration techniques.



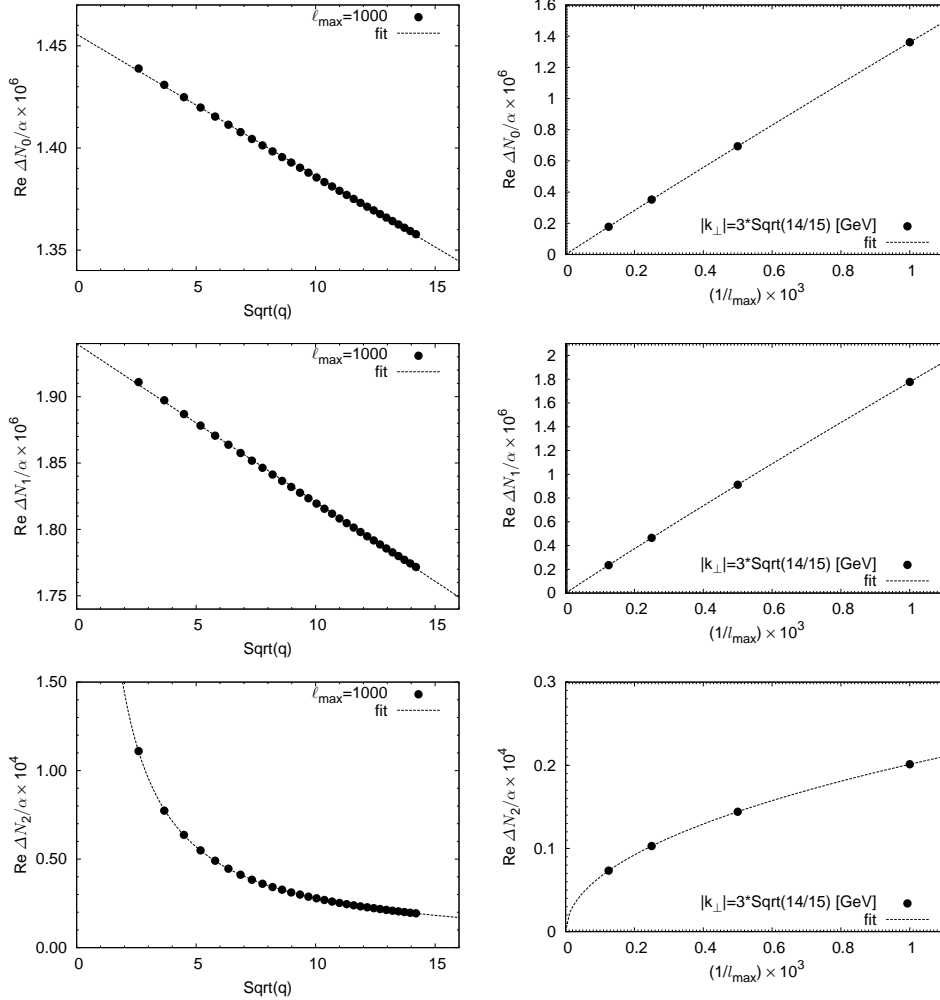


Fig. 10.  $q$  dependence (left panels) and  $l_{\max}$  (right panels) dependence of truncation errors at  $r = 0.8$  (case [a-1]).

## 6. Summary

We investigated the vacuum polarization tensor in constant background magnetic fields based on the Hattori-Itakura's Landau-level summation formula with the appropriate UV subtraction method we constructed. We could reproduce the numerical values computed with the Landau-level summation form consistent with those with known formulae. The Landau-level summation was truncated and we estimated the truncation error in a range of the parameter sets for muons and electrons. In very strong magnetic fields  $eB = m_{\pi}^2 - 10m_{\pi}^2$ , we could evaluate the form factors with practically acceptable accuracy in the limited kinematic region  $1 \text{ [GeV]} < |\mathbf{k}_{\perp}|$ ,

Table 2. Fit results for Eqs. (51)-(53).

Case	[a-1]	[b-1]	[c-1]
$c_0$	$1.820 \times 10^{-3}$	$1.794 \times 10^{-2}$	$1.636 \times 10^{-1}$
$d_0$	$-2.748 \times 10^{-4}$	$-7.002 \times 10^{-3}$	$-1.174 \times 10^{-1}$
$e_0$	$1.828 \times 10^{-3}$	$1.877 \times 10^{-2}$	$3.132 \times 10^{-1}$
$c_1$	$2.425 \times 10^{-3}$	$2.380 \times 10^{-2}$	$2.116 \times 10^{-1}$
$d_1$	$-4.720 \times 10^{-4}$	$-1.202 \times 10^{-2}$	$-2.048 \times 10^{-1}$
$e_1$	$2.439 \times 10^{-3}$	$2.513 \times 10^{-2}$	$2.652 \times 10^{-1}$
$c_2$	$-1.324 \times 10^{-3}$	$-1.231 \times 10^{-2}$	$-1.203 \times 10^{-1}$
$d_2$	$1.145 \times 10^{-2}$	$3.609 \times 10^{-2}$	$1.137 \times 10^{-1}$
Case	[a-2]	[b-2]	[c-2]
$c_0$	$4.256 \times 10^{-8}$	$4.196 \times 10^{-7}$	$3.830 \times 10^{-6}$
$d_0$	$-3.105 \times 10^{-11}$	$-7.921 \times 10^{-10}$	$-1.329 \times 10^{-8}$
$e_0$	$4.275 \times 10^{-8}$	$4.391 \times 10^{-7}$	$7.360 \times 10^{-6}$
$c_1$	-	-	$4.959 \times 10^{-6}$
$d_1$	-	-	$-2.324 \times 10^{-8}$
$e_1$	$5.705 \times 10^{-8}$	$5.880 \times 10^{-7}$	$1.076 \times 10^{-5}$
$c_2$	$-3.096 \times 10^{-8}$	$-2.879 \times 10^{-7}$	$-2.820 \times 10^{-6}$
$d_2$	$5.539 \times 10^{-5}$	$1.746 \times 10^{-4}$	$5.505 \times 10^{-4}$

$0 < k_{\parallel}^2 < 4^2$  [GeV<sup>2</sup>] for muons and electrons. This kinematic region is accessible provided by a small invariant mass in the heavy ion collision experiment at RHIC<sup>34</sup> and LHC<sup>35</sup> where such a strong magnetic field exists in the early stage of the heavy ion collision. The propagation of a real or a virtual photon emitted in the early stage of the collision could receive a large asymmetry due to the direction dependent polarization tensor originating from the pair creation phase space suppression due to the Landau-level bound states. Hadronic contributions to the vacuum polarization tensor must be incorporated before phenomenologically applying the propagator to investigate the effect of strong magnetic fields. However we expect that the polarization tensor estimated in this paper is partly applicable to prove the existence of strong magnetic fields via the photon propagation in the heavy ion collisions at LHC experiments.

### Acknowledgments

We thank Koich Hattori and Kazunori Itakura for valuable discussions. The numerical computations have been done with the PC cluster at INSAM (Institute for Nonlinear Science and Applied Mathematics) Hiroshima University. This work is supported in part by JSPS KAKENHI Grant Number 23654091 (Grant-in-Aid for Challenging Exploratory Research).

### Appendix A. Integrals for Eqs. (25)-(27)

We follow the notations given by Ref. 25 except for the dimensionless parameters  $r$  and  $\mu$  (correspondence to Ref. 25 is  $r \leftrightarrow r_{\parallel}^2$ ,  $\mu \leftrightarrow B_r$ ). The analytic expression for

Eq. (25) is

$$F_\ell^n(r, \mu) = \begin{cases} \frac{1}{\sqrt{\mathcal{D}}} \ln \left| \frac{a - c - \sqrt{\mathcal{D}}}{a - c + \sqrt{\mathcal{D}}} \right| & (r < s_-^{\ell n}) \\ \frac{2}{\sqrt{|\mathcal{D}|}} \left[ \arctan \left( \frac{b + 2a}{\sqrt{|\mathcal{D}|}} \right) - \arctan \left( \frac{b - 2a}{\sqrt{|\mathcal{D}|}} \right) \right] & (s_-^{\ell n} < r < s_+^{\ell n}), \\ \frac{1}{\sqrt{\mathcal{D}}} \left[ \ln \left| \frac{a - c - \sqrt{\mathcal{D}}}{a - c + \sqrt{\mathcal{D}}} \right| + 2\pi i \right] & (s_+^{\ell n} < r) \end{cases} \quad (\text{A.1})$$

$$s_\pm^{\ell n} \equiv \frac{1}{4} \left( \sqrt{1 + 2\ell\mu} \pm \sqrt{1 + 2(\ell + n)\mu} \right)^2, \quad (\text{A.2})$$

where  $a \equiv r$ ,  $b \equiv -n\mu$ ,  $c \equiv 1 - r + (2\ell + n)\mu$ , and  $\mathcal{D} \equiv b^2 - 4ac$ .

Eqs. (26) and (27) are given by

$$G_\ell^n(r, \mu) = \frac{1}{2r} [\Xi_\ell^n(\mu) + n\mu F_\ell^n(r, \mu)], \quad (\text{A.3})$$

$$H_\ell^n(r, \mu) = \frac{1}{r} \left[ 2 + \frac{n\mu}{2r} \Xi_\ell^n(\mu) + \frac{b^2 - 2ac}{2a} F_\ell^n(r, \mu) \right], \quad (\text{A.4})$$

$$\Xi_\ell^n(\mu) \equiv \ln \left| \frac{1 + 2\ell\mu}{1 + 2(\ell + n)\mu} \right|. \quad (\text{A.5})$$

When evaluating these functions numerically, the naive implementation causes a loss of significant figures near  $r = 0$ . We use 8th order Taylor expansion forms when  $|r/(n\mu)| < 10^{-3}$  for  $n > 0$  and  $|r/(1 + 2\ell\mu)| < 10^{-3}$  for  $n = 0$ .

## Appendix B. Form factors with $q = 0$

When  $q = 0$  case we can integrate  $z$  analytically for Eq. (7) using the residue theorem and the reflection formula of the DiGamma function. The expression for  $N_1$  has been obtained in Ref. 28. We give similar expressions for  $N_0$  and  $N_2$  in order to compare the numerical values with the Landau-level summation formula with  $q = 0$  as a consistency check.

After integrating for  $z$  in  $N_0$  we obtain

$$\begin{aligned}
 N_0 = & -\frac{\alpha}{4\pi} \left\{ \int_{-1}^1 dv \frac{1}{2} \left[ -2v^2 - 2(1-v^2) \ln(2\mu) \right. \right. \\
 & - \left( 1 + v \left( \frac{S_0^1(v; r, \mu)}{\mu} - 1 \right) \right) \Psi \left( \frac{S_{K+1}^1(v; r, \mu)}{2\mu} \right) \\
 & - \left. \left( 1 - v \left( \frac{S_0^1(-v; r, \mu)}{\mu} - 1 \right) \right) \Psi \left( \frac{S_{K+1}^1(-v; r, \mu)}{2\mu} \right) \right] \\
 & + 2 \sum_{k \geq 0}^K \left[ \frac{1}{a} \left\{ -2b + (c-a) b F_k^1(r, \mu) \right. \right. \\
 & \left. \left. + (b^2 - a^2 - ac + a) G_k^1(r, \mu) \right\} + b H_k^1(r, \mu) \right] \Big\}, \quad (\text{B.1})
 \end{aligned}$$

where  $a \equiv r$ ,  $b \equiv -\mu$ , and  $c \equiv 1 - r + (2k+1)\mu$ . The shift integer  $K$  is given by

$$K = \begin{cases} -\text{Ceiling}[A_0^1] & (|\mu/(2r)| < 1 \text{ and } A_0^1 \leq 0) \\ -1 & (\text{otherwise}) \end{cases}, \quad (\text{B.2})$$

where  $S_\ell^n$  and  $A_\ell^n$  are given by Eq. (28) and Eq. (32) respectively.

Similarly we have

$$\begin{aligned}
 N_1 = & -\frac{\alpha}{4\pi} \left\{ \int_{-1}^1 dv (1-v^2) \left[ -\ln(2\mu) - \Psi \left( \frac{S_{K+1}^0(v; r, \mu)}{2\mu} \right) \right] \right. \\
 & \left. - \mu (F_0^0(r, \mu) - H_0^0(r, \mu)) + \sum_{k \geq 0}^K 2\mu (F_k^0(r, \mu) - H_k^0(r, \mu)) \right\}, \quad (\text{B.3})
 \end{aligned}$$

$$K = \begin{cases} -\text{Ceiling}[A_0^0] & (A_0^0 \leq 0) \\ -1 & (\text{otherwise}) \end{cases}, \quad (\text{B.4})$$

$$\begin{aligned}
 N_2 = & -\frac{\alpha}{4\pi} \left\{ \int_{-1}^1 dv \frac{1}{2} \left[ -1 - 3v^2 - 2(1-v^2) \ln(2\mu) + 2 \frac{S_0^0(r, \mu)}{\mu} \right. \right. \\
 & - 2 \left( \frac{S_0^0(v; r, \mu)}{\mu} \right)^2 \Psi \left( \frac{S_{1+J+1}^0(v; r, \mu)}{2\mu} \right) \\
 & + \frac{S_0^1(v; r, \mu)}{\mu} \left( \frac{S_0^1(v; r, \mu)}{\mu} - 2 \right) \Psi \left( \frac{S_{K+1}^1(v; r, \mu)}{2\mu} \right) \\
 & + \frac{S_0^1(-v; r, \mu)}{\mu} \left( \frac{S_0^1(-v; r, \mu)}{\mu} - 2 \right) \Psi \left( \frac{S_{K+1}^1(-v; r, \mu)}{2\mu} \right) \Big] \\
 & + \sum_{j \geq 0}^J 2 \left[ \left( 2 - \frac{4r}{3} \right) \frac{1}{\mu} - 4(j+1) + 4(j+1)^2 \mu F_{j+1}^0(r, \mu) \right] \\
 & \left. + \sum_{k \geq 0}^K 2 \left[ - \left( 2 - \frac{4r}{3} \right) \frac{1}{\mu} + 2(2k+1) - 4k(k+1) \mu F_k^1(r, \mu) \right] \right\}, \quad (\text{B.5})
 \end{aligned}$$

$$J = \begin{cases} -\text{Ceiling}[A_1^0] & (A_1^0 \leq 0) \\ -1 & (\text{otherwise}) \end{cases}, \quad (\text{B.6})$$

$$K = \begin{cases} -\text{Ceiling}[A_0^1] & (|\mu/(2r)| < 1 \text{ and } A_0^1 \leq 0) \\ -1 & (\text{otherwise}) \end{cases}. \quad (\text{B.7})$$

**Appendix C. Zero field limit of the imaginary parts of Eqs. (B.1) and (B.3) with  $q = 0$**

The vacuum polarization tensor in vacuum is written by

$$\Pi(k^2) = \frac{\alpha}{3\pi} \left\{ \frac{1}{3} + \left( 2 + \frac{1}{y} \right) \left[ \sqrt{1/y - 1} \cot^{-1} \left( \sqrt{1/y - 1} \right) - 1 \right] \right\} \quad (\text{C.1})$$

for  $y < 1$  and

$$\Pi(k^2) = \frac{\alpha}{3\pi} \left\{ \frac{1}{3} + \left( 2 + \frac{1}{y} \right) \left[ \sqrt{1 - 1/y} \tanh^{-1} \left( \sqrt{1 - 1/y} \right) - 1 - i \frac{\pi}{2} \sqrt{1 - 1/y} \right] \right\}, \quad (\text{C.2})$$

for  $1 < y$  with  $y \equiv k^2/(2m)^2$ . The imaginary part is thus

$$\text{Im}\Pi(k^2) = -\frac{\alpha}{6} (2 + 1/y) \sqrt{1 - 1/y}. \quad (\text{C.3})$$

The zero field limit for the imaginary parts of Eqs. (B.1) and (B.3) can be taken as follows.

$$\begin{aligned} \lim_{\epsilon B \rightarrow 0} \text{Im}N_0 &= \lim_{\epsilon B \rightarrow 0} \left[ -\frac{\alpha}{4\pi} \text{Im} \left\{ 2 \sum_{k \geq 0}^K \left[ \frac{1}{a} \left\{ -2b + (c - a)bF_k^1(r, \mu) \right. \right. \right. \right. \\ &\quad \left. \left. \left. + (b^2 - a^2 - ac + a)G_k^1(r, \mu) \right\} + bH_k^1(r, \mu) \right] \right\} \right] \\ &= \lim_{\Delta\beta \rightarrow 0} \left[ -\frac{\alpha}{4\pi} \frac{\pi}{2} \sum_{k \geq 0}^{\frac{1-1/r}{\Delta\beta}} \left( 1 + \frac{1}{r} + \beta_k \right) \frac{\Delta\beta}{\sqrt{\beta_k}} \right], \quad (\text{C.4}) \end{aligned}$$

where  $\Delta\beta \equiv 2\mu/r$  and  $\beta_k \equiv 1 - 1/r - k\Delta\beta$ . This is the rectangular approximation of integration and the limit leads

$$\begin{aligned} \lim_{\epsilon B \rightarrow 0} \text{Im}N_1 &= -\frac{\alpha}{4\pi} \frac{\pi}{2} \int_0^{1-1/r} \left( 1 + \frac{1}{r} + \beta \right) \frac{d\beta}{\sqrt{\beta}} \\ &= -\frac{\alpha}{6} (2 + 1/r) \sqrt{1 - 1/r} = \text{Im}\Pi(k_{\parallel}^2). \quad (\text{C.5}) \end{aligned}$$

Similarly we have

$$\begin{aligned}
\lim_{\epsilon B \rightarrow 0} \text{Im} N_1 &= \lim_{\epsilon B \rightarrow 0} \left[ -\frac{\alpha}{4\pi} \text{Im} \left[ \mu \sum_{k \geq 0}^K (2 - \delta_{0k}) (F_k^0(r, \mu) - H_k^0(r, \mu)) \right] \right] \\
&= \lim_{\Delta\beta \rightarrow 0} \left[ -\frac{\alpha}{4\pi} \frac{\pi}{2} \sum_{k \geq 0}^{\frac{1-1/r}{\Delta\beta}} (2 - \delta_{0k}) \left( \frac{1 - \beta_k}{\sqrt{\beta_k}} \right) \Delta\beta \right] \\
&= -\frac{\alpha}{4\pi} \pi \int_0^{1-1/r} \left( \frac{1 - \beta}{\sqrt{\beta}} \right) d\beta \\
&= -\frac{\alpha}{6} (2 + 1/r) \sqrt{1 - 1/r} = \text{Im}\Pi(k_{\parallel}^2). \tag{C.6}
\end{aligned}$$

#### Appendix D. Three term recurrence for $C_\ell^n$ and $dC_\ell^n/d\eta$

When we evaluate  $C_\ell^n$  and  $dC_\ell^n/d\eta$  for a large Landau level ( $n, m$ ) with a naive implementation using the three term recurrence formula for Laguerre polynomials, we encounter arithmetic overflow or underflow in double precision arithmetic. In order to tame the numerical overflow and underflow we employ a modified recurrence formula with rescaling and quadruple precision arithmetic.

We define  $f_\ell^n$  and  $df_\ell^n$  satisfying the following recurrence formula;

$$f_0^n = 1, \quad f_{-1}^n = 0, \quad df_0^n = 0, \quad df_{-1}^n = 0, \tag{D.1}$$

$$f_\ell^n = (\alpha_\ell^n f_{\ell-1}^n + \beta_\ell^n f_{\ell-2}^n) \gamma_\ell^n, \tag{D.2}$$

$$df_\ell^n = (\alpha_\ell^n df_{\ell-1}^n + \beta_\ell^n df_{\ell-2}^n - f_{\ell-1}^n) \gamma_\ell^n, \tag{D.3}$$

$$\alpha_\ell^n = (2\ell + n - 1 - \eta), \tag{D.4}$$

$$\beta_\ell^n = (1 - \ell - n) \sqrt{(\ell - 1)/(\ell - 1 + n)}, \tag{D.5}$$

$$\gamma_\ell^n = \sqrt{\ell/(\ell + n)}/\ell, \tag{D.6}$$

for  $1 \leq \ell$ .  $\eta$  is the argument of  $C_\ell^n$  and  $dC_\ell^n/d\eta$ .  $f_\ell^n$  and  $df_\ell^n$  are proportional to  $\sqrt{\ell!/((\ell + n)!)} L_\ell^n(\eta)$  and its derivative respectively. When either of  $|f_\ell^n|$  or  $|df_\ell^n|$  takes a value larger than  $10^{100}$  or smaller than  $10^{-100}$  during the recurrence, intermediate states,  $(f_\ell^n, f_{\ell-1}^n, f_{\ell-2}^n, df_\ell^n, df_{\ell-1}^n, df_{\ell-2}^n)$ , are rescaled by multiplying the inverse of  $\max(|f_\ell^n|, |df_\ell^n|)$  or  $\min(|f_\ell^n|, |df_\ell^n|)$  and the scaling factor is stored for later use below.

The coefficients  $C_\ell^n$  and  $dC_\ell^n/d\eta$  are derived by

$$C_\ell^n(\eta) = (h_n f_\ell^n)^2, \tag{D.7}$$

$$\frac{dC_\ell^n}{d\eta}(\eta) = \left[ 2 (h_n f_\ell^n) (h_n df_\ell^n) - (h_n f_\ell^n)^2 \right] + n (g_n f_\ell^n)^2, \tag{D.8}$$

$$h_n = \begin{cases} e^{-(\eta + \sum_{k \geq 1}^n \log(k) - 2 \sum_{j \geq 1}^{N_{\text{scale}}} \log(S_j) - n \log(\eta))/2} & (\text{for } \eta > 1) \\ e^{-(\eta + \sum_{k \geq 1}^n \log(k) - 2 \sum_{j \geq 1}^{N_{\text{scale}}} \log(S_j))/2} \eta^n & (\text{for } \eta \leq 1) \end{cases}, \quad (\text{D.9})$$

$$g_n = \begin{cases} e^{-(\eta + \sum_{k \geq 1}^n \log(k) - 2 \sum_{j \geq 1}^{N_{\text{scale}}} \log(S_j) - (n-1) \log(\eta))/2} & (\text{for } \eta > 1) \\ e^{-(\eta + \sum_{k \geq 1}^n \log(k) - 2 \sum_{j \geq 1}^{N_{\text{scale}}} \log(S_j))/2} \eta^{n-1} & (\text{for } \eta \leq 1) \end{cases}, \quad (\text{D.10})$$

where  $S_j$ 's are the rescaling factors stored during the recurrence. Finally the coefficients  $C_\ell^n$  and  $dC_\ell^n/d\eta$  are converted to double precision numbers.

## References

1. S. L. Adler, *Annals Phys.* **67**, 599 (1971).
2. W. Tsai and T. Erber, *Phys. Rev. D* **10**, 492 (1974).
3. V. I. Ritus, *J. Sov. Laser Res.* **6**, 497 (1985).
4. W. Dittrich and H. Gies, In *Frontier Tests of QED and Physics of the Vacuum*, Edited by E. Zavattini, D. Bakalov, and C. Rizzo, Heron Press (Sofia, Hungary), 1998., p.29 [hep-ph/9806417].
5. J. I. Weise and D. B. Melrose, *Phys. Rev. D* **73**, 045005 (2006).
6. V. N. Baier and V. M. Katkov, *Phys. Lett. A* **374**, 2201 (2010) [arXiv:0912.5250 [hep-ph]]; *Phys. Rev. D* **75**, 073009 (2007) [hep-ph/0701119].
7. W. Tsai, *Phys. Rev. D* **10**, 2699 (1974).
8. W. Tsai and T. Erber, *Phys. Rev. D* **12**, 1132 (1975).
9. L. F. Urrutia, *Phys. Rev. D* **17**, 1977 (1978).
10. D. B. Melrose and R. J. Stoneham, *Nuovo Cim. A* **32**, 435 (1976); *J. Phys. A: Math. Gen.* **10**, 1211 (1977).
11. C. Schubert, *Nucl. Phys. B* **585**, 407 (2000) [hep-ph/0001288]; *Nucl. Phys. B* **585**, 429 (2000) [hep-ph/0002276]; H. Gies and C. Schubert, *Nucl. Phys. B* **609**, 313 (2001) [hep-ph/0104077].
12. H. Gies and L. Roessler, *Phys. Rev. D* **84**, 065035 (2011) [arXiv:1107.0286 [hep-ph]]; H. Gies and K. Klingmuller, *Phys. Rev. D* **72**, 065001 (2005) [hep-ph/0505099].
13. V. Skokov, A. Yu. Illarionov, V. Toneev, *Int. J. Mod. Phys. A* **24** (2009) 5925 [arXiv:0907.1396 [nucl-th]].
14. D. N. Voskresensky and N. Y. Anisimov, *Sov. Phys. JETEP* **51**, 13(1980) [*Zh. Eksp. Teor. Fiz.* **78**, 28 (1980)].
15. For a review, see K. Fukushima, arXiv:1209.5064 [hep-ph].
16. K. Fukushima, D. E. Kharzeev, H. J. Warringa, *Phys. Rev. D* **78** (2008) 074033 [arXiv:0808.3382 [hep-ph]].
17. H. -U. Yee, arXiv:1303.3571 [nucl-th].
18. K. Tuchin, *Phys. Rev. C* **83** (2011) 017901 [arXiv:1008.1604 [nucl-th]].
19. K. Tuchin, *Phys. Rev. C* **82** (2010) 034904 [Erratum-ibid. *C* **83** (2011) 039903] [arXiv:1006.3051 [nucl-th]].
20. S. Turbide, C. Gale and R. J. Fries, *Phys. Rev. Lett.* **96** (2006) 032303 [hep-ph/0508201].
21. R. Chatterjee, E. S. Frodermann, U. W. Heinz and D. K. Srivastava, *Phys. Rev. Lett.* **96** (2006) 202302 [nucl-th/0511079].
22. B. Layek, R. Chatterjee and D. K. Srivastava, *Phys. Rev. C* **74** (2006) 044901 [nucl-th/0605019].
23. B. Z. Kopeliovich, H. J. Pirner, A. H. Rezaeian and I. Schmidt, *Phys. Rev. D* **77** (2008) 034011 [arXiv:0711.3010 [hep-ph]].

24 *K.-I. Ishikawa, D. Kimura, K. Shigaki, A. Tsuji*

24. B. Z. Kopeliovich, A. H. Rezaeian and I. Schmidt, Nucl. Phys. A **807** (2008) 61 [arXiv:0712.2829 [hep-ph]].
25. K. Hattori and K. Itakura, Annals Phys. **330**, 23 (2013) [arXiv:1209.2663 [hep-ph]].
26. T. Inagaki, D. Kimura and T. Murata, Prog. Theor. Phys. **111**, 371 (2004) [hep-ph/0312005].
27. T. Inagaki, D. Kimura and T. Murata, Int. J. Mod. Phys. A **20**, 4995 (2005) [hep-ph/0307289].
28. F. Karbstein, L. Roessler, B. Dobrich and H. Gies, Int. J. Mod. Phys. Conf. Ser. **14**, 403 (2012) [arXiv:1111.5984 [hep-ph]].
29. K. Kohri and S. Yamada, Phys. Rev. D **65**, 043006 (2002) [astro-ph/0102225].
30. N. M. Temme, J. Appl. Math. Phys. (ZAMP) **41**, 114 (1990).
31. A. Deaño, E. J. Huertas, F. Marcellán, arXiv:1301.4266 [math.CA], to be published in J. Math. Anal. Appl. (2013).
32. T. Ooura, Numerical Automatic Integrator for Improper Integral program using Double-Exponential Quadrature formula, <http://www.kurims.kyoto-u.ac.jp/~ooura/index.html>
33. K. Fukushima, Phys. Rev. D **83** (2011) 111501 [arXiv:1103.4430 [hep-ph]].
34. A. Adare *et al.* [PHENIX Collaboration], Phys. Rev. C **81** (2010) 034911 [arXiv:0912.0244 [nucl-ex]].
35. B. Alessandro *et al.* [ALICE Collaboration], J. Phys. G **32** (2006) 1295.